Title	Characterization of primary organic aerosol from domestic wood, peat, and coal burning in Ireland
Authors	Lin, Chunshui;Ceburnis, D.;Hellebust, Stig;Buckley, Paul;Wenger, John C.;Canonaco, Francesco;Prévôt, André Stephan Henry;Huang, Ru-Jin;O'Dowd, Colin D.;Ovadnevaite, Jurgita
Publication date	2017-08-17
Original Citation	Lin, C., Ceburnis, D., Hellebust, S., Buckley, P., Wenger, J., Canonaco, F., Prévôt, A. S. H., Huang, R.-J., O'Dowd, C., Ovadnevaite, J. (2017) 'Characterization of primary organic aerosol from domestic wood, peat, and coal burning in Ireland', Environmental Science and Technology, 51(18), pp.10624-10632. doi:10.1021/acs.est.7b01926
Type of publication	Article (peer-reviewed)
Link to publisher's version	10.1021/acs.est.7b01926
Rights	© 2017, American Chemical Society. All rights reserved. This document is the Accepted Manuscript version of a Published Work that appeared in final form in Environmental Science and Technology, after peer review and technical editing by the publisher. To access the final edited and published work see http://pubs.acs.org/doi/abs/10.1021/acs.est.7b01926
Download date	2024-03-28 10:51:00
Item downloaded from	https://hdl.handle.net/10468/4921

Article

Characterization of primary organic aerosol from domestic wood, peat, and coal burning in Ireland

Chunshui Lin, Darius Ceburnis, Stig Michael Hellebust, Paul Buckley, John Charles Wenger, Francesco Canonaco, Andre S.H. Prevot, Ru-Jin Huang, Colin O'Dowd, and Jurgita Ovadnevaite

Just Accepted

ACS Publications

Characterization of primary organic aerosol from domestic wood, peat, and coal burning in Ireland

Chunshui Lin[a,b], Darius Ceburnis[a], Stig Hellebust[c], Paul Buckley[c], John Wenger[c], Francesco Canonaco[d], André Stephan Henry Prévôt[d], Ru-Jin Huang[a,b,d,], Colin O'Dowd[a,*], and Jurgita Ovadnevaite[a]*

[a]School of Physics and Centre for Climate and Air Pollution Studies, Ryan Institute, National University of Ireland Galway, University Road, H91CF50, Galway, Ireland

[b] State Key Laboratory of Loess and Quaternary Geology and Key Laboratory of Aerosol Chemistry and Physics, Institute of Earth Environment, Chinese Academy of Sciences, 710061, Xi'an, China

[c]Department of Chemistry and Environmental Research Institute, University College Cork, T23XE10, Cork, Ireland

[d]Laboratory of Atmospheric Chemistry, Paul Scherrer Institute (PSI), 5232 Villigen, Switzerland

1   ABSTRACT: An Aerosol Chemical Speciation Monitor (ACSM) was deployed to study the

2   primary non-refractory submicron particulate matter emissions from burning of commercially

3   available solid fuels (peat, coal, and wood) typically used in European domestic fuel stoves.

4   Organic mass spectra (MS) from burning wood, peat, and coal were characterized and inter-

5   compared for factor analysis against ambient data. The reference profiles characterized in this

6   study were used to estimate the contribution of solid fuel sources, along with oil combustion, to

7   ambient pollution in Galway, Ireland using the multilinear engine (ME-2). During periods

8   influenced by marine air masses, local source contribution had dominant impact and non-sea

9   spray primary organic emissions comprised 88% of total organic aerosol mass, with peat burning

10   found to be the greatest contributor (39%), followed by oil (21%), coal (17%), and wood (11%).

11   In contrast, the resolved oxygenated organic aerosol (OOA) dominated the aerosol composition

12   in continental air masses, with contributions of 50%, compared to 12% in marine air masses. The

13   source apportionment results suggest that the use of domestic solid fuels (peat, wood, and coal)

14   for home heating is the major source of evening/night-time particulate pollution events despite

15   their small use.

16   **1. INTRODUCTION**

17   Ambient particulate matter (PM) adversely affects human health[1, 2] and has been credited with a

18   more positive effect on climate through directly scattering or absorbing solar radiation and

19   indirectly acting as cloud condensation nuclei[3], both leading to a partial negation of global

20   warming induced by greenhouse gas emissions. In Ireland, domestic coal burning was the cause

21   of numerous air pollution events in the 1980s which led to increased mortality rates[4]. The

22   introduction of the ban on marketing, sale, and distribution of bituminous (smoky) coal in Dublin

23   in 1990, which was subsequently extended to urban areas with a population over 15,000, resulted

24   in significant reductions in black smoke concentration and noticeable improvements in air

25   quality[5, 6]. However, a recent study in the city of Cork, Ireland[7], using polar organic compounds

26   to estimate the contribution of domestic solid fuel (DSF) combustion, indicates that despite the

27   ban on bituminous coal, DSF is still the major source of $PM_{2.5}$ organic carbon (0.6-23.7 µg/m^3)

28   during winter (contributing around 75% to total $PM_{2.5}$). Thus, the ban on bituminous coal alone

29   may not be enough since peat and wood emit similar or higher amounts of PM when burned. In

30   fact, according to the report from International Energy Agency (2013)[8], the annual consumption

31   of bituminous coal in Ireland was 404 kt in 2013, while annual peat consumption was 611 kt,

32   which makes peat one of the most commonly used solid fuels. In contrast, the annual

33   consumption of wood for domestic heating was only 34 kt in 2015. Different types of DSF have

34   different emissions factors that are dependent on the type of fuel and burning conditions[9-11].

35   However, developing a way to identify and evaluate the contribution of DSF burning to

36   particulate matter with high time resolution is limited.

37   The identification of specific marker compounds in aerosol particles produced from different

38   solid fuels and the use of markers for subsequent evaluation of the DSF contribution to airborne

39   pollution has been reported by Kourtchev et al.[7] Polar organic maker compounds (i.e.

40   levoglucosan, galactosan, and mannosan) determined by GC/MS and levoglucosan/OC ratio

41   derived from combustion experiments of coal, peat, and wood were used to identify and evaluate

42   their contributions to ambient PM[7]. However, GC/MS suffers from low time resolution (6 h) and

43   levoglucosan/OC ratio might differ greatly under different burning conditions which limit this

44   tracer approach. Recently, the Aerosol Mass Spectrometer (AMS), which determines the

45   chemical composition and concentration of submicron aerosols on-line and at high time

46   resolution has proved to be a robust tool for evaluating the contribution of various sources[12-17].

47   Based on thermal vaporization and electron impact, AMS classifies OA by mass spectrometric

48   fingerprint rather than individual specific marker compounds[18]. Several major components of

49   OA have been identified through positive matrix factorization (PMF) analysis of AMS mass

50   spectra such as hydrocarbon-like (HOA), biomass burning (BBOA), oxygenated (OOA) and

51   several other primary OA[19-21]. Direct AMS measurement of OA from various primary emissions

52   can help understand the MS signatures of different primary OA sources and thus help the

53   interpretation of AMS data. Emissions from motor vehicles[22, 23], meat cooking[24], and solid

54   fuels[10, 25, 26] have been intensively studied and compared in terms of their AMS mass spectral

55   signatures. However, the source profiles may differ with fuel types and combustion conditions,

56   and relevant studies are very scarce, hindering the efforts for a better apportionment of sources

57   with PMF-AMS. Healy et al.[25] and Dall'Osto et al.[26] carried out a series of experiments on wood,

58   smokeless coal and peat burning in an open-door grate using ATOFMS (aerosol time-of-flight

59   mass spectrometer) and HR-ToF-AMS (high -resolution time-of-flight aerosol mass

60   spectrometer), respectively, which provides high mass resolution characterization of emitted PM.

61   Wang et al.[9] characterized OA formation during pulverized coal combustion in a drop-tube

62   furnace. Zhou et al.[11] studied the evolution of OA from burning different types of coal in a

63   typical Chinese stove using an Aerosol Chemical Speciation Monitor (ACSM, a compact version

64   of AMS)[27]. However, to the best of our knowledge, direct Q-ACSM measurements and

65   comparison of domestic wood, peat, and coal burning have not been reported which should get

66   more attention for their significant impacts on air quality in Ireland and other places (e.g. the UK

67   and Finland) where these fuels are popular for domestic heating[6, 7, 25, 26].

68   In this study, seven solid fuel samples including dry wood (15%-20% moisture, DW), wet

69   wood (>20% moisture, WW), dry raw peat (DP), wet raw peat (WP), peat briquettes (PB),

70   bituminous (smoky) coal (SC) and ovoids (smokeless, based on anthracite) coal (SLC) were

71   burned in a typical residential stove in Ireland. Characterization of PM emitted from burning

72   these samples was conducted using an ACSM. OA was found to be the major contributor to the

73   total sub-micron non-refractory (NR-PM$_1$) aerosol particles. Mass spectral signatures of OA

74   from each fuel type were obtained at unit mass resolution and compared. These signatures were

75   used to apportion ambient OA measured by ACSM in Galway, Ireland to estimate the relative

76   contribution of each type of fuel to air pollution and characterize their emission and formation

77   process by comparing the influence of continental and marine air masses.

78   **2. EXPERIMENTAL SECTION**

79   **Solid-fuel types.** Wood (oak), raw peat, peat briquettes, bituminous (smoky) coal and

80   smokeless coal ovoids were purchased locally in County (Co.) Tipperary, where the burning

81   experiments were performed. Peat products are locally produced while smoky coal is imported

82   from Colombia (78% of the coal in Ireland is imported from Colombia in 2014; SEAI 2016).

83   Smokeless coal (ovoids) is purchased from ArignaBiofuels (based in Ireland) where coal is

84   roasted, blended with other biomass products and briquetted as ovoids. Stored, dried wood had a

85   moisture content less than 20%. Wet wood had a moisture content from 20% up to 40%. Peat is

86   an accumulation of partially decayed vegetation and is the first step for the formation of coal.

87   Raw peat is cut from peatlands while peat briquettes are compressed peat[28]. Raw peat was dry

88   when purchased and was exposed to the outdoor atmosphere to achieve wet raw peat. Smoky

89   coal and smokeless coal were directly burned as they are more water resistant.

90   **Fingerprinting experiment set-up.** The solid fuel burning experiments were performed using

91   a solid fuel stove located in a cottage in Co. Tipperary from January 16 to 21 2016 with an

92   average ambient temperature of 6 $\pm$3 ^{o}C and RH of 92$\pm$5%. A schematic of the stove and

93   sampling system is provided in Scheme S1. Each type of sampling fuel was continuously burned

94   for at least 1 hours with a total use of each type of fuel >5kg. The stove was cleared of residue

95   following combustion of each fuel sample. An ACSM (Aerodyne Research Inc.) was used to

96   characterize the chemical composition of the NR-PM$_1$ and obtain unique mass spectral signatures

97   of aerosols produced from burning each of the solid fuels. In the ACSM[27], nafion dried

98   submicron particles sampled through the inlet are deposited on the heated surface (600 ^{o}C), and

99   only the NR-PM$_1$ are vaporized and ionized by the ion source. The resulting ions are analyzed by

100 quadrupole mass spectrometer. Black carbon and other refractory components are not analyzed

101 by ACSM. The time resolution of ACSM for ambient measurement is usually set at ~15-30

102 minutes due to the low concentration, while in this direct fuel combustion measurement, it was

103 set at ~1 minute (1 set of sample and filter cycle) for the high aerosol emission (10-500 μg/m^3)

104 during the sampling period. The emissions from the 1 h burning were averaged to get the relative

105 mass contribution and mass spectral signatures of organic aerosol for each type of fuel.

106 **Ambient aerosol measurements in Galway.** The ambient aerosol measurements were

107 conducted in the National University of Ireland Galway's Center of Climate and Air Pollution

108 Studies (53.28^{o}N and 9.06^{o}W) from 17th October 2015 to 23rd November 2015. This site is

109 located adjacent to and east off the main urban residential area and at least 200 meters away from

110 the main road to avoid the direct influence from traffic. Ambient air was drawn from a height of

111 around 6 m above the ground through a tube at a flow rate at 3 LPM. A sub-stream of ~85

112 ml/min was analyzed by ACSM at a time resolution of 30 minutes. Meteorological data recorded

113 at the engineering building (1 km from the monitoring site) was used to compare and analyze the

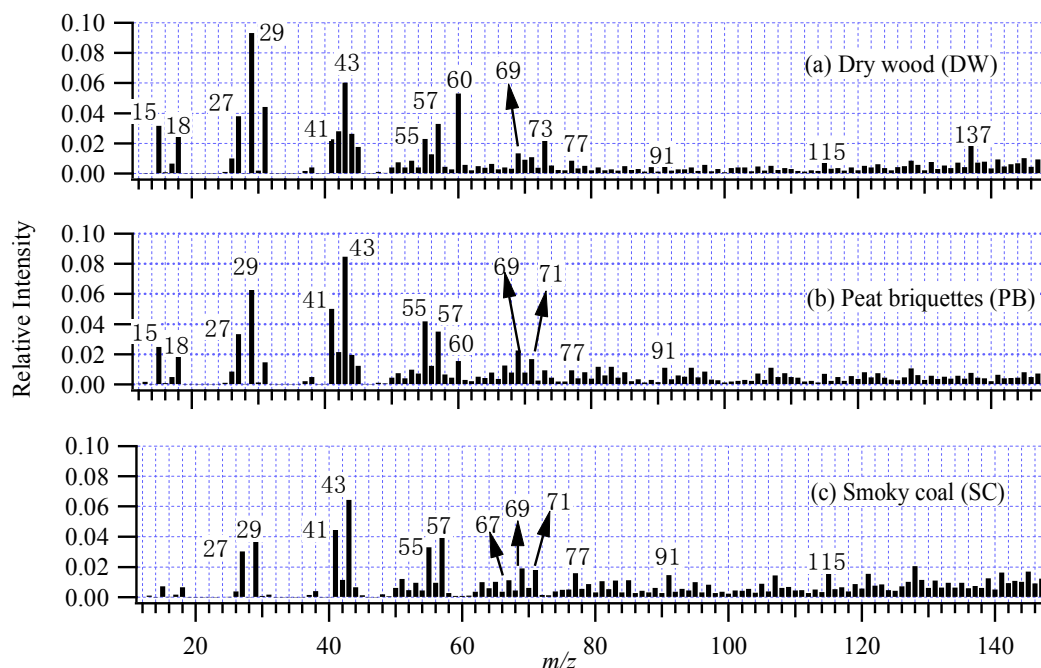114 origin and transport of aerosol in this study.

115

116   **Data analysis.** In this study, we employ ME-2[29, 30, 31] within the SoFi software package (version

117   6.1), an Igor-based software, for source apportionment. A detailed description of ME-2 and the

118   software package can be found in Canonaco et al.[29]. Briefly, in a typical PMF algorithm where a

119   measured matrix X can be deconvolved into two matrices (G and F) and the remaining residue

120   matrix (E), multiple combinations of G and F due to rotational ambiguity can lead to

121   mathematically meaningful but not interpretable PMF solutions especially when factors show

122   temporal covariations. An *a-value* approach within ME-2 has been successfully used to explore

123   the rotational ambiguity for online and offline data set where users can direct the algorithm

124   towards environmentally reasonable rotations by constraining reference factor profiles (currently

125   the case) or time series based on priori information.[17, 32, 33] The *a-value* determines the extent to

126   which a reference profile is allowed to vary (e.g. an *a-value* of 0.1 allows a variability of 10%).

127   In this study, the pollution events mostly happened during eveing/nighttime, indicating their

128   emission sources from domestic heating. Thus, we conducted the source apportionment by

129   constraining the primary components, i.e., oil (HOA), peat, coal, and wood using the *a-value*

130   approach and allowed for one additional free factor representing OOA. HOA reference profile,

131   taken from Crippa et al.[21], usually represents emission profile from traffic.[34, 35] However, oil

132   burning has similar particulate emissions to that of traffic emission in terms of mass spectra as

133   indicated in the diesel burning work by Schneider et al.[23] and the vehicles chase study by

134   Canagaratna et al.[22] Actually, oil burning for domestic heating is quite popular in Galway,

135   Ireland (around 85% of the non-natural gas and non-electricity households) based on the census

136   data from Central Statistics Office on the households by the type of central heating (CSO)[36]

137   (Figure S1). The night time peaks of HOA (Figure 4a and 4b) indicates its source from domestic

138   heating, HOA is, therefore, denoted as oil burning thereafter. The *a value* of 0.1 (*a value* of 0-0.2

139   was explored, more information is provided in Section **OA source apportionment**) was used for

140   all primary factors (oil, peat, coal, and wood).

141   **3. RESULTS AND DISCUSSION**

142   **Relative fraction of solid fuels burning NR-PM$_1$ emissions.** Organics constitute the largest

143   fraction of total NR-PM$_1$ emissions from burning fuels (e.g. ~98% for dry wood, ~91% for peat

144   briquettes, and ~94% smoky coal) except for the smokeless coal (~26%) (Figure S2). For the

145   latter, chloride is the major component of the aerosol particles, with a value of about 53%,

146   followed by organics (26%), sulfate (11%), and ammonium (8%). Burning conditions have

147   minor effects on the relative contribution of ACSM species by comparing dry and wet wood, dry

148   and wet raw peat. In contrast, the compositions of fuel type result in differences in contributions

149   to NR-PM$_1$ mass between different types of fuels. For example, wood burning emissions contain

150   little sulfate and little ammonium (~0.3%) while all types of peat burning emissions have higher

151   levels of sulfate, with around 5% of the total NR-PM$_1$ mass being sulfate for peat briquettes.

Figure 1. Normalized mass spectra of organics from the combustion of (a) dry wood; (b) peat briquettes; (c) smoky coal.

ACSM mass spectra profiles of different fuels. Averaged normalized ACSM unit mass resolution (UMR) mass spectra (MS) of OA particles obtained for dry wood, peat, and coal are shown in Figure 1. All three MS are dominated by C_nH_{2n+1} (29, 43, 57, 71…) and C_nH_{2n-1} (27, 41, 55, 69…), indicating the large contribution from saturated alkanes, alkenes, and also possible cycloalkanes in the primary OA emissions from wood, peat, and coal. However, the MS profile patterns and signals at specific m/z (e.g. m/z 60) of different fuels vary significantly corresponding to the composition of the fuels. For example, the most prominent ion in wood burning aerosol MS profile is the signal at m/z (mass to charge ratio) 29, followed by m/z 43 while m/z 43 is the most abundant ion in peat emissions, followed by m/z 29. In contrast, m/z 43 and m/z 41 are the most abundant ions in coal emissions MS. In addition, there was a relatively

164 higher contribution from heavier ions (>100) in the coal emission spectra most likely from PAH

165 emissions if compared to the peat and wood spectra.

166 **Wood.** The prominent signals at *m/z* 29 and 43 in wood emissions (Figure 1a) are consistent

167 with the previous reports using HR-ToF-AMS.[24] The large presence of CHO^+ and $C_2H_3O^+$ in

168 HR-ToF-AMS are found to be responsible for the high signal at *m/z* 29 and *m/z* 43,

169 respectively[24]. Mass fragments at *m/z* 60 are often regarded as marker fragments for wood

170 burning aerosols[37] which mainly arise from the thermal decomposition of cellulose, the pyrolysis

171 of which produces levoglucosan. The electron impact ionization of levoglucosan shows intense

172 signals at *m/z* 60.[26] Fragment *m/z* 44 (CO_2^+, strongly influenced by di or polycarboxylic acids), a

173 marker for OOA,[38] which arises together with *m/z* 18 (which is set to equal to *m/z* 44 in the

174 fragmentation table as in the Q-AMS) contributes to around 2% of total BBOA signal[39, 40].

175 Fragment *m/z* 29 has the highest fraction of the signal in the dry wood profile. However, it is not

176 a unique marker for wood burning due to its presence in all other fuel profiles. These

177 characteristics are consistent with other UMR MS of OA from pine burning and PMF results of

178 ambient OA data.[10, 37] Wet wood profile shows a higher contribution from larger *m/z* fragments

179 especially at *m/z* 137 (Figure S3) which may be due to the fact that wet wood has a lower

180 burning temperature which leads to incomplete combustion. Despite the differences between dry

181 wood and wet wood profile, wood marker fragments *m/z* 60, 73 and 137 are still prominent. The

182 MS signal fractions of *m/z* >80 for dry wood are 31% which implies that primary OA from wood

183 burning contains high molecular weight organic compounds. This high fraction is consistent with

184 the previous fingerprinting experiment reported by He et al.[24] in which high signal fractions of

185 *m/z* >100 could reach 13%. However, the absolute amount is strongly influenced by the

186   transmission function applied in the ACSM in which small errors in the higher m/z range can

187   cause the behavior of slowly increasing calculated signal at m/z above 100.

188   **Peat.** MS of primary OA from peat shows the highest signal fraction at m/z 43 (Figure 1b),

189   which is consistent with the HR-ToF-AMS measurement of open grate peat burning[26] and ToF-

190   ACSM measurement of peat burning in closed chamber[41]. Ions at m/z 43 are dominated by $C_3H_7^+$

191   in peat emissions while $C_2H_3O^+$ dominate the same nominal ions in wood emissions in HR-ToF-

192   AMS[26]. $C_xH_y^+$ type ions make up 71 % of peat MS, which implies high fraction of hydrocarbon

193   in peat emissions[26]. In addition, typical aromatic ion series at m/z 77 and 91 are present in the

194   peat MS and are more prominent than that in wood MS. The presence of m/z 60 in peat MS

195   profiles is due to the incomplete decay of vegetation which contains cellulose.[42] Cellulose is one

196   of the most common chemical substances that exist in peat.[42] Although these ion series in peat

197   profile are not as prominent as in the wood profile, ions at m/z 60 are enough to distinguish the

198   peat MS profile from coal and oil whose formation involves a complete decay of vegetation. For

199   example, HOA from traffic typically has the most prominent peak at m/z 57, characteristic of

200   saturated hydrocarbons, but no signal at m/z 60.[20, 43] High similarity in MS profiles for dry, wet

201   raw peat and peat briquettes (R^2>0.95) can be observed which suggests that the state of the peat

202   (raw, wet, shredded and compressed into briquettes) does not make a difference to the OA mass

203   spectra (Figure S4). The MS signal fractions of m/z > 80 for peat are 34% which is slightly

204   higher than wood, indicating high molecular weight compounds are forming in peat.

205   **Coal.** The burning of smoky coal visibly produces a larger amount of black carbon than

206   smokeless coal. However, the mass spectral signatures of smoky and smokeless coal appear very

207   similar (Figure S5), both with large contribution from heavier ions. The similarity in MS patterns

208   between smoky and smokeless coal indicates that the compositions in ovoids responsible for the

209   emission of primary OA are similar to that of smoky coal. The strongest peak in coal MS is the

210   signal at *m/z* 43, followed by *m/z* 41 (Figure 1c). This is similar to peat and consistent with a

211   previous HR-ToF-AMS measurement of emissions from open grate coal burning.[26] $C_xH_y^+$ type

212   ions dominate the MS of coal with a fraction of 71% which is the same as peat MS profile.[26]

213   Coal is formed through a process called "coalification"[44] when peat is physically and chemically

214   altered as a result of bacterial decay, compaction, heat and time. No signal at *m/z* 60 was

215   observed for smoky coal MS (Figure 1c) which might be due to the complete decomposition of

216   cellulose in the formation of coal. In contrast, *m/z* 60 is slightly elevated in ovoids MS which

217   might be due to its complex composition that contains biomass. The absence of *m/z* 60

218   distinguishes smoky coal MS from contemporary biomass burning. In addition, the signal at *m/z*

219   57 is slightly higher than *m/z* 55 in coal profile while the opposite is the case for peat, indicating

220   that coal has more saturated hydrocarbon than peat. Further, fragments at *m/z* 77, 91 and 115 are

221   stronger in coal MS than in peat MS likely due to the high fraction of aromatic compounds in

222   coal. The signal fractions of *m/z* > 80 are 51% which is significantly higher than wood and peat.

223   **Differences between ACSM profiles and implications for PMF analysis.** The differences

224   between the MS shown in Figure 1 are compared by plotting the relative differences of

225   individual m/z values compared to peat (i.e. (f(m/z, wood/coal) - f(m/z, peat))/f(m/z, peat),

226   Figure S6). The peat MS was chosen as the reference MS due to the fact peat is the middle

227   evolution state between wood and coal. Wood and peat MS show moderate similarity with the

228   correlation value R^2 of 0.69 (Table S2). Differences at values of m/z 29, 31, 41, 60, 73, 83, 96,

229   and 137 are mainly responsible for the discrepancy. Higher values of m/z 29, 31, 60, 73, 137

230   (positive relative difference for wood) are observed for wood while higher values of m/z 41, 83,

231   96 (negative relative difference) are observed for peat. Coal and peat MS also show moderate
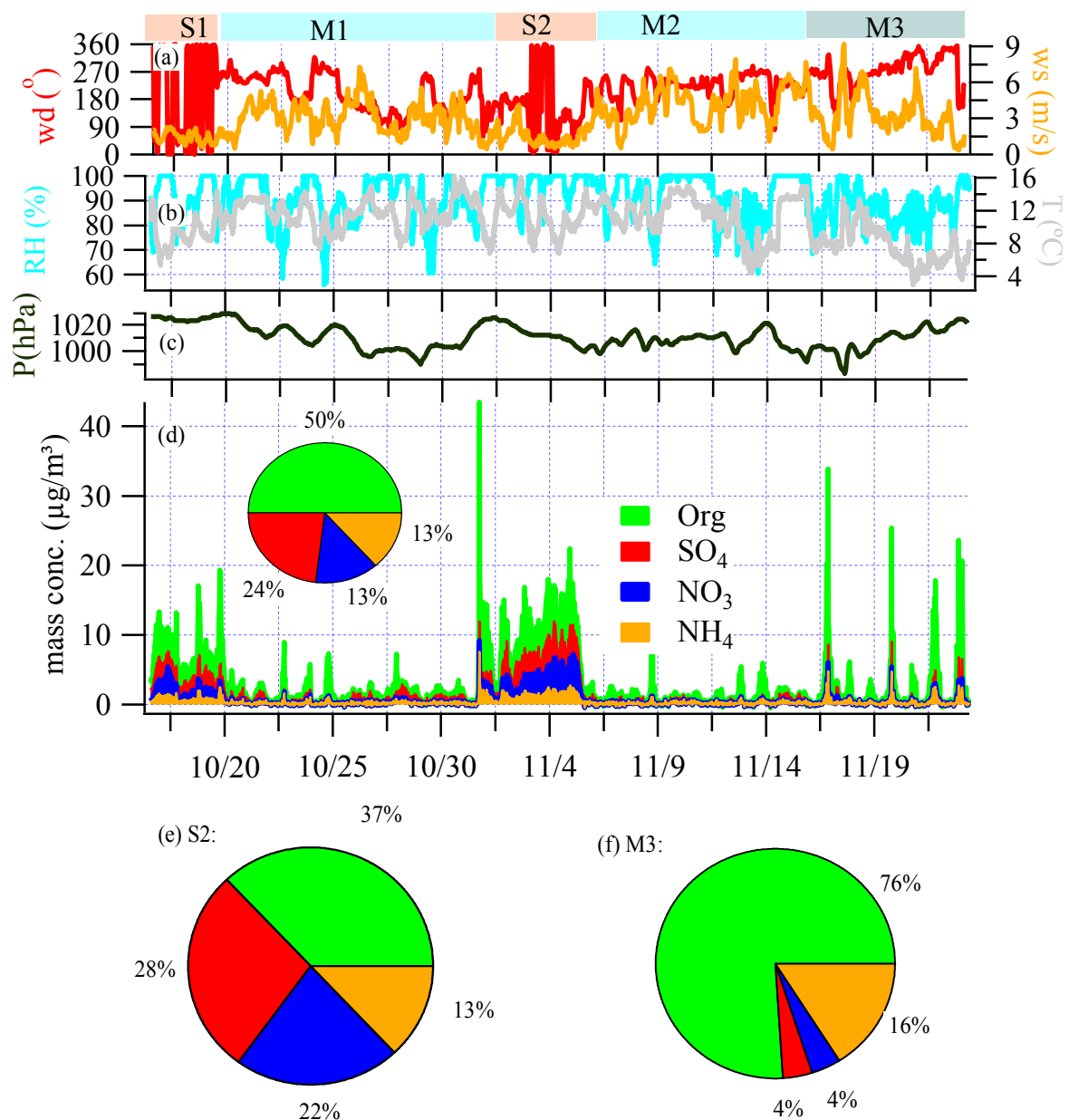
232   similarity with R^2 being 0.77. Higher values at m/z 29, 31, 45, 60, 73 for peat and higher values

233   at m/z > 115 for coal contribute mainly to the discrepancy. The differences in intensities at the

234   m/z values mentioned above are expected to play an important role in PMF to separate OA

235   emissions from wood, peat, and coal.

236   For the comparison between MS profiles of all the burning sources in this study and PMF

237   factors of ambient measurement from literature, R^2 were calculated and summarized in Table S2.

238   The dry and wet raw peat MS shows a good inter-correlation with R^2 being 0.98 which was

239   higher than that between dry wood and wet wood (R^2=0.91), indicating wood burning emissions

240   are more influenced by moisture. Smoky coal and smokeless coal show the poorest inter-

241   correlation (R^2=0.78) which is in part due to the production process of smokeless coal from

242   smoky coal that leaves out most of the volatile content in smoky coal responsible for the high

243   smoke output. In fact, the signal fractions in the range *m/z* > 80 for smokeless coal MS are 40.9%

244   which is less than that of smoky coal (51.3%). The discrepancy in the MS between smoky coal

245   and smokeless coal can also be explained by complicated compositions of ovoids which is

246   blended with biomass (www.arignabiofuels.ie). This might also be the reason that the correlation

247   coefficient between smokeless coal and peat could reach 0.92. In this regard, it is hard to

248   separate peat and smokeless coal in factor analysis of the ambient dataset. Peat briquettes MS is

249   better correlated with PMF factor BBOA (taken from Ng et al.[43]) (mean R^2=0.88) than dry wood

250   (R^2=0.77) which implies that in areas where peat is widely used (e.g. Ireland and the UK)

251   extreme care is required to separate peat and BBOA since they have similar MS and usually

252   show temporal covariation as domestic heating fuels. Peat shows moderate correlation (mean

253   R^2=0.8) with HOA (taken from Crippa et al.[21]), but elevated signal at *m/z* 60 for peat should be

254   enough to distinguish them in PMF analysis. Wood and HOA shows a bad correlation (mean

255   R^2=0.25) which means that wood burning emissions can be easily separated from HOA in factor

256   analysis of the ambient dataset.

257

258   **Ambient measurement of NR-PM$_1$ in Galway, Ireland.**   An overview of the NR-PM$_1$

259   components (organics, nitrate, sulfate, and ammonium) in Galway during early winter (from

260   October 17th to November 23rd, 2015) is shown in Figure 2 as well as meteorological parameters

261   (wind direction, wind speed, relative humidity, and temperature). During the measurement

262   period, the temperatures were mild, with an average of 10.6 ± 2.6 ^{o}C ranging from 3 ^{o}C to 16 ^{o}C.

263   The ambient relative humidity had a mean value of 90.8 ± 8.8 %, ranging from 56 % to 100 %.

264   The wind mainly blew from the southwest (46 % of the time) with a mean wind velocity of 3.1 ±

265   1.6 m/s ranging from 0.4 to 9.2 m/s. The ACSM yielded a range of NR-PM$_1$ concentrations from

266   0.1 to 43.5 µg/m^3, with a low mean value of 3.4 ± 4.5 µg/m^3 mainly due to the frequent influence

267   of clean marine air masses. However, under certain meteorological conditions of continental air

268   masses (periods S1 and S2) and low wind speed (< 2 m/s), a high concentration of NR-PM$_1$ can

269   build up throughout the day, with an average of 7.8 µg/m^3 and 11.2 µg/m^3 for S1 and S2,

270   respectively. Even with marine air masses and associated low wind speed (M3), high peak NR-

271   PM$_1$ concentration (34 µg/m^3, 10 times mean NR-PM$_1$ value) can be seen in the

272   evening/nighttime, indicating the large emissions from domestic heating in Galway. And a very

273   low background concentration of lower than 1 µg/m^3 was observed during the daytime of the

274   period M3 despite high pollution at night. Thus, it is insightful to analyze the composition during

275   different periods.

276   On average, the NR-PM$_1$ mass mainly comprised of OA (50%), followed by sulfate (24%),

277   ammonium (13%), and nitrate (13%) for the entire measurement period in Galway (Figure 2d).

278   However, under different meteorological conditions, their fractions vary significantly. During

279   stagnant time periods (S2) with continental air masses, the pollution levels were elevated

280   throughout the day and the fraction of secondary inorganic aerosols (sulfate, nitrate, and

281   ammonium) increased to around 63% (Figure 2e), indicating a regional source. In contrast,

282   during marine time periods, OA alone accounts for 76% of total NR-PM$_1$ mass (Figure 2f). The

283   recurring evening/nighttime pollution events with OA being the dominant component underline

284   the importance of source apportionment of OA.
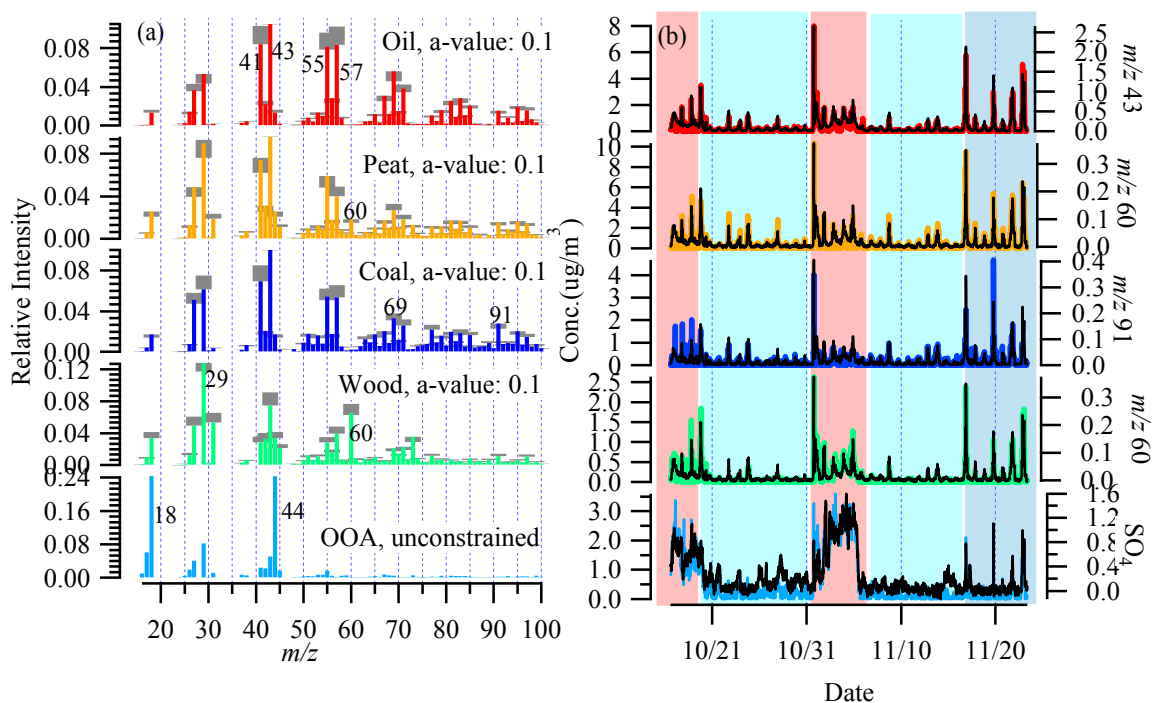
Figure 2. Time series of (a) wind direction (wd) and wind speed (ws); (b) relative humidity (RH) and temperature (T); (c) pressure (P); and (d) submicron species i.e. organics, sulfate, ammonium, and nitrate; inset pie chart shows average composition for the entire study; and pie chart contribution of submicron species during selected periods (e) S2; and (f) M3; The colors

289　　and characters on the top of the graph represent the different air masses classifications (light red:

290　　stagnant continental (S1 and S2); light green: marine with high wind speed (M1 and M2; dark

291　　green: marine with low wind speed (M3); back trajectory analysis for the whole periods is shown

292　　in Figure S11).

293　　　**OA source apportionment.** For source apportionment of OA, we take advantage of ME-2

294　　which can direct the PMF analysis to environmentally reasonable solutions by constraining the

295　　priori ACSM derived source profiles of peat, coal, and wood, as well as oil (HOA) from Crippa

296　　et al.[21] An *a-value* of 0.1 (i.e. 10% variation in profile) was applied due to the fact that most

297　　primary OA was freshly-emitted, with peak concentrations occurring at the early nighttime and

298　　thus should have small variation from the ACSM derived fingerprints. Due to the lack of

299　　possible tracer marker for each type of domestic fuel combustions, the best *a-value* will be

300　　further investigated as indicated in Elser et al.[17] As illustrated in Figure 3a, a 5-factor solution

301　　including four constrained primary factors and one additional unconstrained OOA is found to be

302　　the environmentally reasonable solution. Further increase of the number of factors leads to

303　　uninterpretable factors (Figure S7). The time series of four primary factors (Figure 3b) show

304　　similar temporal variation due to the similar emission time from domestic heating activities

305　　during the evening which was also the reason why ME-2 is necessary to separate pre-constrained

306　　factors to estimate the contribution of candidate sources. Otherwise, highly mixed and un-

307　　meaningful factors would be achieved with a totally unconstrained PMF (Figure S8) and thus, an

308　　unconstrained PMF would be unable to estimate the contribution of the different combustion

309　　fuels to the air pollution. In contrast, the OOA could be easily resolved both in constrained and

310　　unconstrained PMF due to its time series distinct from primary factors. OOA is characterized

311　　with a prominent signal at *m/z* 44 and has a high correlation with sulfate (R^2=0.83). The OOA

312   time series show a relatively constant high level during periods S1 and S2, indicating the

313   importance of OOA formation under these conditions. However, during periods M1, M2, and

314   M3, some evening peaks of OOA can also be observed, indicating an additional contribution

315   from a more local and evening/nighttime production process. Unlike OOA, the resulting time

316   series of primary factors only show elevated evening/nighttime pollution levels, corresponding to

317   emission time.

318   **Figure 3.** (a) Factor profiles (mass spectra) of 5-factor ME-2 solution. The a-value method

319   within SoFi was applied (matrix with *m/z* up to 100 was used for PMF). Oil burning profile is

320   from ambient data PMF-derived hydrocarbon-like organic aerosol (HOA)[21]. Peat, wood, and coal

321   reference profiles are from previous fingerprinting experiments. Grey bar in the back represents

322   reference profile employed. (b) And the factor time series (color coded with the same periods of

323   S1, M1, S2, M2, and M3 in Figure 2) of source apportionment and comparison of primary

324   factors with typical ACSM fragments (HOA vs m/z 43 (R^2=0.88); Peat vs m/z 60 (R^2=0.84); Coal

325   vs m/z 91 (R^2=0.63); Wood vs m/z 60 (R^2=0.79)) and comparison of secondary factor (OOA)

326   with an external source of sulfate (R^2=0.83).

327   When running ME-2 using the *a-value* approach on ACSM datasets, the selection of best *a*

328   value is critical. An *a* value that is too small (i.e. very tightly constrained) might not give enough

329   freedom to the unconstrained factor (e.g. OOA) while a large *a* value might lead to inter-factor

330   mixing. Thus, an optimized *a* value need to be explored in ME-2. Previous work by Elser et al.[17]

331   suggests the selection criteria of using factor-tracer correlation to find the best *a* value

332   corresponding solution that best describes the organic aerosols. A combination of different *a*

333   values for a specific factor can be derived using this method. However, in cases where the

334   constrained factors' corresponding tracer data are not available, we assume a same *a* value for all

335   constrained factors. To explore the influence of *a* value, *a* value of 0, 0.05, 0.1, and 0.2 were run

336   in ME-2. The constrained factors' relative fraction and the correlation between the unconstrained

337   OOA and sulfate are found to be affected by *a* value differently (Figure S10). The factors'

338   relative contribution to total OA for oil, coal, and wood burning remain nearly unchanged for

339   this *a* value range (0-0.2). In contrast, OOA fraction decreases sharply from 45% to 35% as *a*

340   value of increases from 0 to 0.1 but slowly from 35% to 34% as *a* value increases from 0.1 to 0.2

341   while peat burning fraction increases from 21% (*a* value of 0) to 32% (*a* value of 0.1) and

342   decreases to 28% (*a* value of 0.2). R^2 between the OOA and sulfate increases from 0.71 to 0.83

343   as the *a* value increase from 0 to 0.1 and starts to level off after 0.1. Thus, 0.1 is found to be the

344   most optimized *a* value because it can give enough freedom to OOA and prevent further mixing
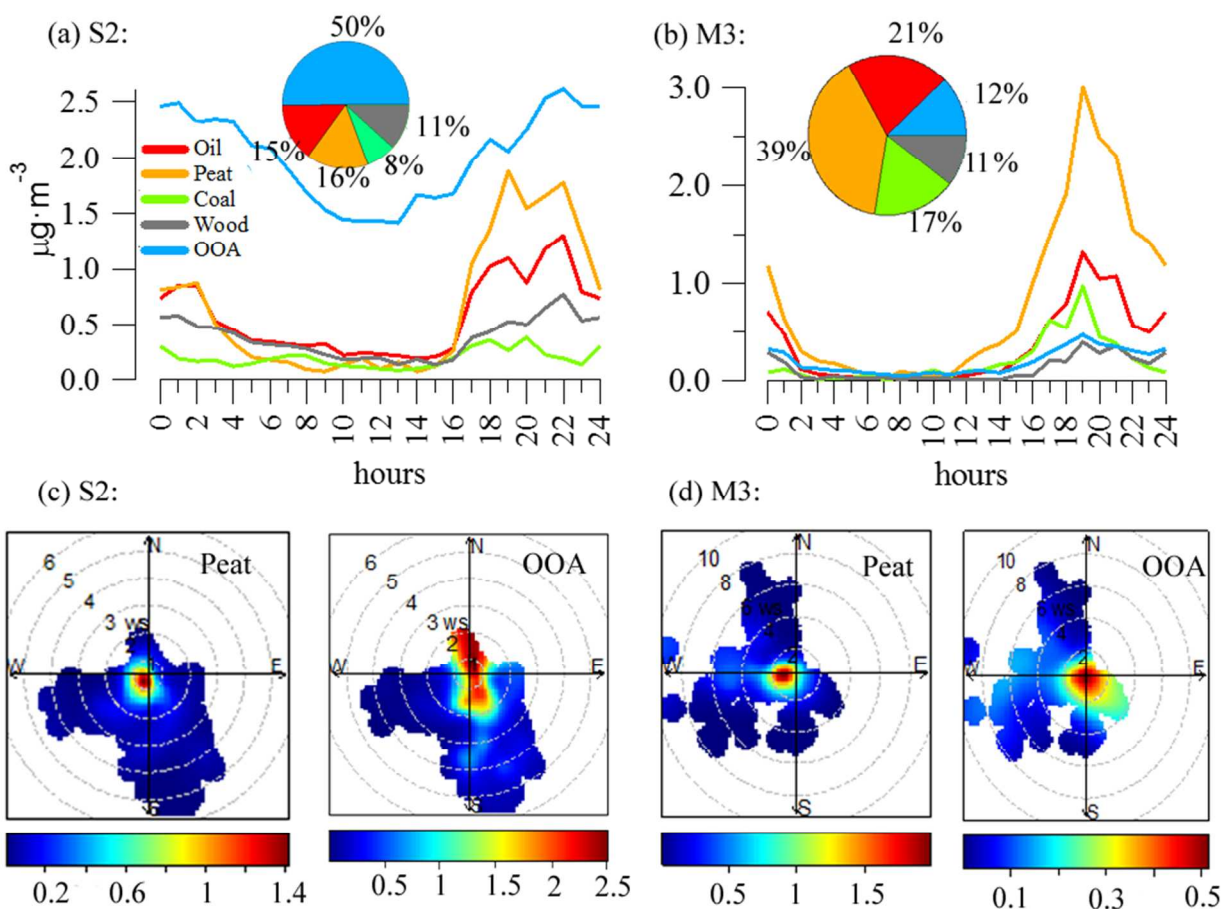
345   between factors by increasing the *a* value. It is also important to note that peat is always the

346   largest primary fraction with the same *a* value.

347   **Local vs. regional OA sources.** During the measurement periods, the frequent marine air

348   masses bring a very clean background OA level (<0.1 μg/m^3) which provide a perfect chance to

349   study the anthropogenic pollutants especially for the local sources. In addition, occasional

350   continental air masses bring the opportunity to study the regional OA sources from the UK

351   and/or mainland Europe. The relationship between resolved OA factors and meteorology is,

352   therefore, demonstrated by comparing two distinct pollution patterns corresponding to

353   continental and marine air masses (Figure S11). Continental air masses and marine air masses

354   alternated during the measurement period and led to different contributions of OA factors, as

355   well as diurnal patterns especially for OOA. As shown in Figure 4 (a), OOA is the major

356   component of OA in continental air masses (S2; 50%), and its diurnal cycle shows higher

357   concentration during the night than day which might be due to the influence of planetary

358   boundary layer that's shallower during night and higher during the day. Wind roses of OOA

359   during S2 show that higher OOA concentrations are related to air masses from the north and

360   southeast side rather than the west side of measurement location, indicating its origin might

361   come from mainland Europe or the UK rather than the ocean (Figure 4c). In contrast, in the

362   marine air masses (i.e. M3 period), OOA only comprises 12% of total OA (Figure 4b), and the

363   diurnal cycle of it shows a peak at evening/nighttime which coincides with primary factors,

364   indicating a possible nighttime OOA formation process of the condensation of semi-volatile

365   organic matter emitted from fuel combustion[47]. In addition, the wind roses of OOA (Figure 4d)

366   during M3 show no preference for wind direction but for low wind speed which might be

367   required for the formation process as semi-volatile organic matter dissipate more quickly with

368　high wind speed. The wind rose of OOA between S2 and M3 shows a clear different pattern

369　indicating the difference in transport and formation of OOA under different meteorological

370　conditions. Similarly, inorganic aerosols (sulfate, nitrate, and ammonium) also show obvious

371　peaks during M3 nighttime which should also come from primary emissions or fast night time

372　formation (Figure 2).

373　　Unlike OOA, all primary factors (oil, peat, coal, and wood burning), show peak concentrations

374　at early night (at around 19:00) and very low concentrations (<0.5 $\mu g/m^3$) during the day (8:00-

375　16:00, sunrise at around 8:00 and sunset at around 16:00 during the measurement period),

376　corresponding to their emission time and locally produced nature. Primary OA contributes

377　around 50 % during S2 and 88% during M3, indicating its importance for air pollution over the

378　wintertime, especially during marine periods. Peat burning contributes 39% during M3 and 16%

379　during S2 (Figure 4a and 4b), making it the largest primary contributor to the total ambient OA

380　during cold winter nights in Galway. This is in great contrast to the relatively small usage of peat

381　as indicated by the census data (Figure S1) from Central Statistics Office which shows only

382　around 10% of the non-natural gas and non-electricity households use peat for heating. However,

383　the emission factor profile (Table S1)[45] which indicates a large emission factor and a low net

384　calorific value for peat can help explain the dominance of peat. Similarly, smoky coal has a large

385　emission factor and claim for 17% of total OA mass during M3 when less than 1% of the

386　households report the use of smoky coal for heating probably due to the ban on coal in Galway.

387　In contrast, most households use oil for heating (around 85%), but due to the low emission factor

388　for oil burning, a relatively small fraction (21% during M3) is observed. HOA is usually used to

389　quantify the traffic emissions.[21] However, the time series of HOA in this study show a huge early

390　evening peak (at around 19:00) and absence of a morning rush hour peak (Figure 4a and 4b),

391   which points to its major source from domestic heating activities rather than traffic as reported

392   by previous papers.[34, 35] It is possible that the interference from oil burning due to their similar

393   mass spectra[22,23] and the low mass resolution of ACSM leads to the difficulties in resolving the

394   traffic factor with a low contribution (e.g. <5%), in particular when it co-varies with a source

395   with higher emissions. Previous work by Ulbrich et al. suggests that true components with <5%

396   of the mass are hard to be retrieved accurately using PMF.[46] In contrast to OOA, the wind roses

397   of major primary factor (i.e. peat burning) always show an origin from the west of the

398   measurement site during both S2 and M3 periods which is consistent with the location of the

399   residential area.

Figure 4. Diurnal cycle of resolved factors (i.e. oil, peat, coal, wood, and OOA) during periods
(a) of relatively stagnant and continental air masses (S2) and (b) marine air masses (M3) (insets
are relative contribution of the resolved OA factors); Polar plot of hourly averaged major
component of OA (i.e. peat and OOA; color coded based on concentration of each species in
$\mu g/m^3$) as function of wind speed (radial axis) and wind direction during periods (c) S2 and (d)
M3. Polar plots figures were generated with OpenAir software[48].

ASSOCIATED CONTENT

Supporting Information. Scheme S1 shows combustion and sampling system for solid fuels
using ACSM. Figure S1 shows the households by the type of central heating (oil, peat, coal, and

409   wood) from Central Statistics Office, 2011. Table S1 provides the emission factors and caloric

410   values for oil, peat, coal, and wood. Table S2 provides correlation coefficient (R^2) between

411   ACSM profiles of different sources and PMF factors. Figure S2 shows the relative fraction of

412   ACSM measured species (i.e. organics, sulfate, nitrate, ammonium, and chloride). Figures S3-S5

413   show the mass spectra of each type of fuel under different states. Figure S6 provides relative

414   difference of dry wood and smoky coal MS profile compared to peat at each m/z. Figures S7-S9

415   provide the time series and mass spectra of PMF solutions. Figure S10 provides the relative

416   contribution of the resolved factors and correlation between OOA and sulfate with different *a*

417   values (0-0.2). Figure S11 shows the back trajectory during the measurement period in Galway

418   Ireland. This material is available free of charge via the Internet at http://pubs.acs.org.

419   AUTHOR INFORMATION

420   **Corresponding Author**

421   *Ru-Jin Huang, Phone: +86-(0)29-6233-6275; Email: rujin.huang@ieecas.cn

422   *Colin O'Dowd, Phone: +353-91-49-3306; Email: colin.odowd@nuigalway.ie

423   **Notes**

424   The authors declare no competing financial interest.

430   for providing valuable input into the design and construction of the sampling system. The team

431   from University College Cork would like to acknowledge support from the Environmental

432   Protection Agency and Department of Environment Community and Local Government in

433   Ireland through the SAPPHIRE project (2013-EH-MS.15).

434   REFERENCES

435   1.   Pope, I. C.; Burnett, R. T.; Thun, M. J., Lung cancer, cardiopulmonary mortality, and

436   long-term exposure to fine particulate air pollution. *JAMA* **2002,** *287*, (9), 1132-1141.

437   2.   Sandström, T.; Nowak, D.; van Bree, L., Health effects of coarse particles in ambient air:

438   messages for research and decision-making. *Eur. Respir. J.* **2005,** *26*, (2), 187-188.

439   3.   O'Dowd, C. D.; Facchini, M. C.; Cavalli, F.; Ceburnis, D.; Mircea, M.; Decesari, S.;

440   Fuzzi, S.; Yoon, Y. J.; Putaud, J.-P., Biogenically driven organic contribution to marine aerosol.

441   *Nature* **2004,** *431*, (7009), 676-680.

442   4.   Kelly, I.; Clancy, L., Mortality in a general hospital and urban air pollution. *Irish Med. J.*

443   **1984,** *77*, (10), 322-324.

444   5.   Clancy, L.; Goodman, P.; Sinclair, H.; Dockery, D. W., Effect of air-pollution control on

445   death rates in Dublin, Ireland: an intervention study. *Lancet* **2002,** *360*, (9341), 1210-1214.

446   6.   Goodman, P. G.; Rich, D. Q.; Zeka, A.; Clancy, L.; Dockery, D. W., Effect of Air

447   Pollution Controls on Black Smoke and Sulfur Dioxide Concentrations across Ireland. *J. Air &*

448   *Waste Manage.* **2009,** *59*, (2), 207-213.

449   7.   Kourtchev, I.; Hellebust, S.; Bell, J. M.; O'Connor, I. P.; Healy, R. M.; Allanic, A.;

450   Healy, D.; Wenger, J. C.; Sodeau, J. R., The use of polar organic compounds to estimate the

451   contribution of domestic solid fuel combustion and biogenic sources to ambient levels of organic

452   carbon and PM2.5 in Cork Harbour, Ireland. *Sci. Total Environ.* **2011,** *409*, (11), 2143-2155.

453   8.   International Energy Agency, 2013. Energy balance for Ireland website;

454   http://www.iea.org/statistics/statisticssearch/report/?country=IRELAND&product=Coal&year=2

455   013 (last access: December 2016).

456   9.   Wang, X.; Williams, B.; Wang, X.; Tang, Y.; Huang, Y.; Kong, L.; Yang, X.; Biswas, P.,

457   Characterization of organic aerosol produced during pulverized coal combustion in a drop tube

458   furnace. *Atmos. Chem. Phys.* **2013,** *13*, (21), 10919-10932.

459   10.   Weimer, S.; Alfarra, M. R.; Schreiber, D.; Mohr, M.; Prévôt, A. S. H.; Baltensperger, U.,

460   Organic aerosol mass spectral signatures from wood-burning emissions: Influence of burning

461   conditions and type. *J. Geophys. Res-Atmos.* **2008,** *113*, (10), 304-305.

462   11.   Zhou, W.; Jiang, J.; Duan, L.; Hao, J., Evolution of Submicrometer Organic Aerosols

463   during a Complete Residential Coal Combustion Process. *Environ. Sci. Technol.* **2016**, *50* (14),

464   7861–7869.

465   12.   Jayne, J. T.; Leard, D. C.; Zhang, X.; Davidovits, P.; Smith, K. A.; Kolb, C. E.; Worsnop,

466   D. R., Development of an aerosol mass spectrometer for size and composition analysis of

467   submicron particles. *Aerosol Sci. Technol.* **2000,** *33*, (1-2), 49-70.

468   13.   Canagaratna, M. R.; Jayne, J. T.; Jimenez, J. L.; Allan, J. D.; Alfarra, M. R.; Zhang, Q.;

469   Onasch, T. B.; Drewnick, F.; Coe, H.; Middlebrook, A.; Delia, A.; Williams, L. R.; Trimborn, A.

470   M.; Northway, M. J.; DeCarlo, P. F.; Kolb, C. E.; Davidovits, P.; Worsnop, D. R., Chemical and

471   microphysical characterization of ambient aerosols with the aerodyne aerosol mass spectrometer.

472   *Mass Spectrom. Rev.* **2007,** *26*, (2), 185-222.

473   14.   Middlebrook, A. M.; Bahreini, R.; Jimenez, J. L.; Canagaratna, M. R., Evaluation of

474   Composition-Dependent Collection Efficiencies for the Aerodyne Aerosol Mass Spectrometer

475   using Field Data. *Aerosol Sci. Technol.* **2012,** *46*, (3), 258-271.

476   15.   Carbone, S.; Saarikoski, S.; Frey, A.; Reyes, F.; Reyes, P.; Castillo, M.; Gramsch, E.;

477   Oyola, P.; Jayne, J.; Worsnop, D.; Hillamo, R., Chemical characterization of submicron Aerosol

478   particles in Santiago de Chile. *Aerosol Air Qual. Res.* **2013,** *13*, (2), 462-473.

479   16.   Canonaco, F.; Slowik, J. G.; Baltensperger, U.; Prévôt, A. S. H., Seasonal differences in

480   oxygenated organic aerosol composition: Implications for emissions sources and factor analysis.

481   *Atmos. Chem. Phys.* **2015,** *15*, (12), 6993-7002.

482   17.   Elser, M.; Huang, R. J.; Wolf, R.; Slowik, J. G.; Wang, Q.; Canonaco, F.; Li, G.;

483   Bozzetti, C.; Daellenbach, K. R.; Huang, Y.; Zhang, R.; Li, Z.; Cao, J.; Baltensperger, U.; El-

484   Haddad, I.; André, P., New insights into PM2.5 chemical composition and sources in two major

485   cities in China during extreme haze events using aerosol mass spectrometry. *Atmos. Chem. Phys.*

486   **2016,** *16*, (5), 3207-3225.

487   18.   Zhang, Q.; Jimenez, J. L.; Canagaratna, M. R.; Ulbrich, I. M.; Ng, N. L.; Worsnop, D. R.;

488   Sun, Y., Understanding atmospheric organic aerosols via factor analysis of aerosol mass

489   spectrometry: A review. *Anal. Bioanal. Chem.* **2011,** *401*, (10), 3045-3067.

490   19.   Jimenez, J. L.; Canagaratna, M. R.; Donahue, N. M.; Prevot, A. S. H.; Zhang, Q.; Kroll,

491   J. H.; DeCarlo, P. F.; Allan, J. D.; Coe, H.; Ng, N. L.; Aiken, A. C.; Docherty, K. S.; Ulbrich, I.

492   M.; Grieshop, A. P.; Robinson, A. L.; Duplissy, J.; Smith, J. D.; Wilson, K. R.; Lanz, V. A.;

493   Hueglin, C.; Sun, Y. L.; Tian, J.; Laaksonen, A.; Raatikainen, T.; Rautiainen, J.; Vaattovaara, P.;

494   Ehn, M.; Kulmala, M.; Tomlinson, J. M.; Collins, D. R.; Cubison, M. J.; E.; Dunlea, J.;

495   Huffman, J. A.; Onasch, T. B.; Alfarra, M. R.; Williams, P. I.; Bower, K.; Kondo, Y.; Schneider,

496   J.; Drewnick, F.; Borrmann, S.; Weimer, S.; Demerjian, K.; Salcedo, D.; Cottrell, L.; Griffin, R.;

497   Takami, A.; Miyoshi, T.; Hatakeyama, S.; Shimono, A.; Sun, J. Y.; Zhang, Y. M.; Dzepina, K.;

498   Kimmel, J. R.; Sueper, D.; Jayne, J. T.; Herndon, S. C.; Trimborn, A. M.; Williams, L. R.;

499   Wood, E. C.; Middlebrook, A. M.; Kolb, C. E.; Baltensperger, U.; Worsnop, D. R., Evolution of

500   Organic Aerosols in the Atmosphere. *Science* **2009,** *326*, (5959), 1525-1529.

501   20.   Lanz, V. A.; Pŕev̂ot, A. S. H.; Alfarra, M. R.; Weimer, S.; Mohr, C.; Decarlo, P. F.;

502   Gianini, M. F. D.; Hueglin, C.; Schneider, J.; Favez, O.; D'Anna, B.; George, C.; Baltensperger,

503   U., Characterization of aerosol chemical composition with aerosol mass spectrometry in Central

504   Europe: An overview. *Atmos. Chem. Phys.* **2010,** *10*, (21), 10453-10471.

505   21.   Crippa, M.; Decarlo, P. F.; Slowik, J. G.; Mohr, C.; Heringa, M. F.; Chirico, R.; Poulain,

506   L.; Freutel, F.; Sciare, J.; Cozic, J.; Di Marco, C. F.; Elsasser, M.; Nicolas, J. B.; Marchand, N.;

507   Abidi, E.; Wiedensohler, A.; Drewnick, F.; Schneider, J.; Borrmann, S.; Nemitz, E.;

508   Zimmermann, R.; Jaffrezo, J. L.; Prévôt, A. S. H.; Baltensperger, U., Wintertime aerosol

509   chemical composition and source apportionment of the organic fraction in the metropolitan area

510   of Paris. *Atmos. Chem. Phys.* **2013,** *13*, (2), 961-981.

511   22.   Canagaratna, M. R.; Jayne, J. T.; Ghertner, D. A.; Herndon, S.; Shi, Q.; Jimenez, J. L.;

512   Silva, P. J.; Williams, P.; Lanni, T.; Drewnick, F.; Demerjian, K. L.; Kolb, C. E.; Worsnop, D.

513   R., Chase Studies of Particulate Emissions from in-use New York City Vehicles. *Aerosol Sci.*

514   *Technol.* **2004,** *38*, (6), 555-573.

515   23.   Schneider, J.; Weimer, S.; Drewnick, F.; Borrmann, S.; Helas, G.; Gwaze, P.; Schmid,

516   O.; Andreae, M. O.; Kirchner, U., Mass spectrometric analysis and aerodynamic properties of

517   various types of combustion-related aerosol particles. *Int. J. Mass Spectrom.* **2006,** *258*, (1-3),

518   37-49.

519   24.   He, L. Y.; Lin, Y.; Huang, X. F.; Guo, S.; Xue, L.; Su, Q.; Hu, M.; Luan, S. J.; Zhang, Y.

520   H., Characterization of high-resolution aerosol mass spectra of primary organic aerosol

521   emissions from Chinese cooking and biomass burning. *Atmos. Chem. Phys.* **2010,** *10*, (23),

522   11535-11543.

523   25.   Healy, R. M.; Hellebust, S.; Kourtchev, I.; Allanic, A.; O'Connor, I. P.; Bell, J. M.;

524   Healy, D. A.; Sodeau, J. R.; Wenger, J. C., Source apportionment of PM$_{2.5}$ in Cork

525   Harbour, Ireland using a combination of single particle mass spectrometry and quantitative semi-

526   continuous measurements. *Atmos. Chem. Phys.* **2010,** *10*, (19), 9593-9613.

527   26.   Dall'Osto, M.; Ovadnevaite, J.; Ceburnis, D.; Martin, D.; Healy, R. M.; O'Connor, I. P.;

528   Kourtchev, I.; Sodeau, J. R.; Wenger, J. C.; O'Dowd, C., Characterization of urban aerosol in

529 Cork city (Ireland) using aerosol mass spectrometry. *Atmos. Chem. Phys.* **2013,** *13*, (9), 4997-

530 5015.

531 27. Ng, N. L.; Herndon, S. C.; Trimborn, A.; Canagaratna, M. R.; Croteau, P. L.; Onasch, T.

532 B.; Sueper, D.; Worsnop, D. R.; Zhang, Q.; Sun, Y. L.; Jayne, J. T., An Aerosol Chemical

533 Speciation Monitor (ACSM) for Routine Monitoring of the Composition and Mass

534 Concentrations of Ambient Aerosol. *Aerosol Sci. Technol.* **2011,** *45*, (7), 780-794.

535 28. Eaton, J. M.; McGoff, N. M.; Byrne, K. A.; Leahy, P.; Kiely, G., Land cover change and

536 soil organic carbon stocks in the Republic of Ireland 1851–2000. *Climatic Change* **2008,** *91*, (3-

537 4), 317-334.

538 29. Canonaco, F.; Crippa, M.; Slowik, J. G.; Baltensperger, U.; Prévôt, A. S. H., SoFi, an

539 IGOR-based interface for the efficient use of the generalized multilinear engine (ME-2) for the

540 source apportionment: ME-2 application to aerosol mass spectrometer data. *Atmos. Meas. Tech.*

541 **2013,** *6*, (12), 3649-3661.

542 30. Paatero, P., Least squares formulation of robust non-negative factor analysis. *Chemometr.*

543 *Intell. Lab* **1997,** *37*, (1), 23-35.

544 31. Paatero, P.; Eberly, S.; Brown, S. G.; Norris, G. A., Methods for estimating uncertainty in

545 factor analytic solutions. *Atmos. Meas. Tech.* **2014,** *7*, (3), 781-797.

546 32. Lanz, V. A.; Alfarra, M. R.; Baltensperger, U.; Buchmann, B.; Hueglin, C.; Prévôt, A. S.

547 H., Source apportionment of submicron organic aerosols at an urban site by factor analytical

548 modelling of aerosol mass spectra. *Atmos. Chem. Phys.* **2007,** *7*, (6), 1503-1522.

549   33.   Crippa, M.; Canonaco, F.; Lanz, V. A.; Äijälä, M.; Allan, J. D.; Carbone, S.; Capes, G.;

550   Ceburnis, D.; Dall'Osto, M.; Day, D. A.; DeCarlo, P. F.; Ehn, M.; Eriksson, A.; Freney, E.;

551   Hildebrandt Ruiz, L.; Hillamo, R.; Jimenez, J. L.; Junninen, H.; Kiendler-Scharr, A.;

552   Kortelainen, A. M.; Kulmala, M.; Laaksonen, A.; Mensah, A. A.; Mohr, C.; Nemitz, E.;

553   O'Dowd, C.; Ovadnevaite, J.; Pandis, S. N.; Petäjä, T.; Poulain, L.; Saarikoski, S.; Sellegri, K.;

554   Swietlicki, E.; Tiitta, P.; Worsnop, D. R.; Baltensperger, U.; Prévôt, A. S. H., Organic aerosol

555   components derived from 25 AMS data sets across Europe using a consistent ME-2 based source

556   apportionment approach. *Atmos. Chem. Phys.* **2014,** *14*, (12), 6159-6176.

557   34.   Petit, J. E.; Favez, O.; Sciare, J.; Canonaco, F.; Croteau, P.; Močnik, G.; Jayne, J.;

558   Worsnop, D.; Leoz-Garziandia, E., Submicron aerosol source apportionment of wintertime

559   pollution in Paris, France by double positive matrix factorization (PMF2) using an aerosol

560   chemical speciation monitor (ACSM) and a multi-wavelength Aethalometer. *Atmos. Chem. Phys.*

561   **2014,** *14*, (24), 13773-13787.

562   35.   Poulain, L.; Iinuma, Y.; Müller, K.; Birmili, W.; Weinhold, K.; Brüggemann, E.; Gnauk,

563   T.; Hausmann, A.; Löschau, G.; Wiedensohler, A.; Herrmann, H., Diurnal variations of ambient

564   particulate wood burning emissions and their contribution to the concentration of Polycyclic

565   Aromatic Hydrocarbons (PAHs) in Seiffen, Germany. *Atmos. Chem. Phys.* **2011,** *11*, (24),

566   12697-12713.

567   36.   Central statistical office 2011, Ireland website;

568   http://www.cso.ie/px/pxeirestat/Statire/SelectVarVal/Define.asp?Maintable=CDD41&Planguage

569   =0 (last access: December 2016).

570   37.   Alfarra, M. R.; Prevot, A. S. H.; Szidat, S.; Sandradewi, J.; Weimer, S.; Lanz, V. A.;

571   Schreiber, D.; Mohr, M.; Baltensperger, U., Identification of the mass spectral signature of

572   organic aerosols from wood burning emissions. *Environ. Sci. Technol.* **2007,** *41*, (16), 5770-

573   5777.

574   38.   Duplissy, J.; DeCarlo, P. F.; Dommen, J.; Alfarra, M. R.; Metzger, A.; Barmpadimos, I.;

575   Prevot, A. S. H.; Weingartner, E.; Tritscher, T.; Gysel, M.; Aiken, A. C.; Jimenez, J. L.;

576   Canagaratna, M. R.; Worsnop, D. R.; Collins, D. R.; Tomlinson, J.; Baltensperger, U., Relating

577   hygroscopicity and composition of organic aerosol particulate matter. *Atmos. Chem. Phys.* **2011,**

578   *11*, (3), 1155-1165.

579   39.   Allan, J. D.; Delia, A. E.; Coe, H.; Bower, K. N.; Alfarra, M. R.; Jimenez, J. L.;

580   Middlebrook, A. M.; Drewnick, F.; Onasch, T. B.; Canagaratna, M. R.; Jayne, J. T.; Worsnop, D.

581   R., A generalised method for the extraction of chemically resolved mass spectra from Aerodyne

582   aerosol mass spectrometer data. *J. Aerosol Sci.* **2004,** *35*, (7), 909-922.

583   40.   Allan, J. D.; Jimenez, J. L.; Williams, P. I.; Alfarra, M. R.; Bower, K. N.; Jayne, J. T.;

584   Coe, H.; Worsnop, D. R., Quantitative sampling using an Aerodyne aerosol mass spectrometer 1.

585   Techniques of data interpretation and error analysis. *J. Geophys. Res-Atmos.* **2003,** *108*, (D3),

586   4090-4091.

587   41. Budisulistiorini, S. H.; Riva, M.; Williams, M.; Chen, J.; Itoh, M.; Surratt, J. D.; Kuwata, M.,

588   Light-Absorbing Brown Carbon Aerosol Constituents from Combustion of Indonesian Peat and

589   Biomass. *Environ. Sci. Technol.* **2017,** 51, (8), 4415-4423.

590   42.   Szajdak, L.; Brandyk, T.; Szatylowicz, J., Chemical properties of different peat-moorsh

591   soils from the Biebrza River Valley. *Agronomy Res.* **2007,** *5*, (2), 165-174.

592   43.   Ng, N. L.; Canagaratna, M. R.; Zhang, Q.; Jimenez, J. L.; Tian, J.; Ulbrich, I. M.; Kroll,

593   J. H.; Docherty, K. S.; Chhabra, P. S.; Bahreini, R.; Murphy, S. M.; Seinfeld, J. H.; Hildebrandt,

594   L.; Donahue, N. M.; DeCarlo, P. F.; Lanz, V. A.; Prévôt, A. S. H.; Dinar, E.; Rudich, Y.;

595   Worsnop, D. R., Organic aerosol components observed in Northern Hemispheric datasets from

596   Aerosol Mass Spectrometry. *Atmos. Chem. Phys.* **2010,** *10*, (10), 4625-4641.

597   44.   Ibarra, J.; Munoz, E.; Moliner, R., FTIR study of the evolution of coal structure during

598   the coalification process. *Org. Geochem.* **1996,** *24*, (6), 725-735.

599   45.   TNO 2001: TNO Institute of Environmental Sciences, Energy Research and Process

600   Innovations: CEPMEIP Database, available at http://www.air.sk/tno/cepmeip, Apeldoorn 2001

601   (last access: December 2016).

602   46. Ulbrich, I. M.; Canagaratna, M. R.; Zhang, Q.; Worsnop, D. R.; Jimenez, J. L., Interpretation

603   of organic components from Positive Matrix Factorization of aerosol mass spectrometric data.

604   *Atmos. Chem. Phys.* **2009,** *9*, (9), 2891-2918.

605   47. Tiitta, P.; Leskinen, A.; Hao, L.; Yli-Pirilä, P.; Kortelainen, M.; Grigonyte, J.; Tissari, J.;

606   Lamberg, H.; Hartikainen, A.; Kuuspalo, K.; Kortelainen, A. M.; Virtanen, A.; Lehtinen, K. E.

607   J.; Komppula, M.; Pieber, S.; Prévôt, A. S. H.; Onasch, T. B.; Worsnop, D. R.; Czech, H.;

608   Zimmermann, R.; Jokiniemi, J.; Sippula, O., Transformation of logwood combustion emissions

609   in a smog chamber: formation of secondary organic aerosol and changes in the primary organic

610   aerosol upon daytime and nighttime aging. *Atmos. Chem. Phys.* **2016,** *16*, (20), 13251-13269.

48. Carslaw, D. C.; Ropkins, K., openair — An R package for air quality data analysis. *Environ. Modell. Softw.* **2012,** *27–28*, 52-61.

TOC: